

M. M. Monfared · M. Ayatollahi · S. M. Mousavi

The mixed-mode analysis of a functionally graded orthotropic half-plane weakened by multiple curved cracks

Received: 25 April 2015 / Accepted: 7 August 2015 / Published online: 25 August 2015
© Springer-Verlag Berlin Heidelberg 2015

Abstract The problem of functionally graded orthotropic half-plane with climb and glide edge dislocations is solved. Dislocations are used as the building blocks of defects to model cracks of modes I and II. Following a dislocation-based approach, the problem is reduced to a system of singular integral equations for dislocation density functions on the surfaces of smooth cracks. These integral equations enforce the crack-face boundary conditions and are solved numerically for the dislocation density. The numerical results include the stress intensity factors for several different cases of crack configurations and arrangements.

Keywords In-plane · Stress intensity factors · Functionally graded orthotropic materials · Multiple cracks · Singular integral equations

1 Introduction

Functionally graded materials for high-temperature applications are special components usually made from ceramics and metals. The ceramic in a FGM offers thermal barrier effects and protects the metal from corrosion and oxidation, and the FGM is toughened and strengthened by metallic composition. The stress analysis of functionally graded orthotropic materials with multiple cracks under in-plane loading is of considerable importance in the design of safe structures. This is due to the ever increasing usage of nonhomogeneous orthotropic materials in modern technology. Because of the nature of the techniques used in processing, the graded materials are seldom isotropic. For example, FGMs processed by using a plasma spray technique have generally lamella structure. Such materials would not be isotropic, but orthotropic, with material directions that can be considered perpendicular to one another in an initial approximated. Thus, orthotropic properties should be considered in studying the mechanics of FGMs.

Erdogan [1] investigated fracture behavior of a nonhomogeneous elastic plane with crack. In this paper, the stress fields had singularity in the form of $r^{-1/2}$, r being the distance from the crack tip. Karihaloo [2] solved the problem of a solid under plane strain shear conditions and he extended the dislocation technique to the investigation of stress relaxation round inhomogeneities that are not coplanar. The fracture analysis of doubly periodic arrays of slit-like cracks with stress relaxation process from the crack tips is solved by Karihaloo [3]. In another article [4], he also studied the problem of an infinite elastic medium containing a sequence of cracks with constant distance of vertical separation. Delale and Erdogan [5] obtained the modes I stress intensity factor for a nonhomogeneous medium containing a crack. The integral equations for the problem were obtained. These

M. M. Monfared · M. Ayatollahi (✉)
Faculty of Engineering, University of Zanjan, P. O. Box 45195-313, Zanjan, Iran
E-mail: mo_ayatollahi@yahoo.com; mo.ayatollahi@gmail.com

S. M. Mousavi
Department of Civil and Structural Engineering, Aalto University, PO Box 12100, 00076 Espoo, Finland

equations were solved numerically to determine the stress intensity factor for a crack. The results shown that the effect of Poisson's ratio and consequently that of the thickness constraint on the stress intensity factors are rather negligible and the results are highly affected by the FG parameter. The mixed-mode problem for an interface crack in a nonhomogeneous elastic medium was solved by Delale and Erdogan [6]. Further results for a crack in a nonhomogeneous material were the subject of study by Erdogan et al. [7]. They solved the plane elasticity problem for two bonded half-planes with a crack perpendicular to the interface. In another paper, the axisymmetric crack problem in a nonhomogeneous medium was studied by Ozturk and Erdogan [8]. The main results were the stress intensity factors as a function of the nonhomogeneous parameter for various loading conditions. The mixed-mode stress intensity factor in a nonhomogeneous medium containing an arbitrarily orientated crack was obtained by Konda and Erdogan [9]. Mauge and Kachanov [10] studied the interaction of arbitrarily oriented cracks in an anisotropic elastic solid. Erdogan [11] examined the influence of the material nonhomogeneity on the asymptotic stress state near the crack tips. Chen and Erdogan [12] investigated the problem of the interface crack in a nonhomogeneous coating bonded to a homogeneous substrate. Jin and Batra [13] considered general fracture mechanics problem for functionally graded materials. They showed that the crack-tip fields in FGMs are identical to those in homogeneous materials. Gu and Asaro [14] have analyzed a semi-infinite crack in a functionally graded materials subjected to in-plane loading. They studied the effects of material gradients on the modes I and II stress intensity factors. Crack in an inhomogeneous orthotropic medium was analyzed by Ozturk and Erdogan [15]. Ozturk and Erdogan [16] provided the stress intensity factors for mixed-mode crack problem in an inhomogeneous orthotropic medium. Anlas et al. [17] investigated the crack in plates made of functionally graded materials. They studied cracked FGM plate by using the several different numerical techniques. Huang and Kardomateas [18] studied the modes I and II stress intensity factors in an anisotropic strip with a crack. Dolbow and Gosz [19] proposed the use of interaction energy method for extracting the mixed-mode stress intensity factors for arbitrarily oriented crack in a functionally graded material. Wang et al. [20] studied functionally graded strip weakened by a crack perpendicular to the boundary by dividing a strip into some layer with homogeneous properties along the thickness direction. Guo et al. [21] considered the mode I crack problem for a functionally graded strip. It has been shown that material constants and the geometry parameters have significant effects on the stress intensity factors. Long and Delale [22] studied the plane elasticity problem of an arbitrarily orientated crack in a FGM layer bonded to homogeneous half-plane. It was found that crack length, orientation and the nonhomogeneity parameter of the layer have a significant effect on the fracture of the FGM layer. The study of dynamic behavior of a finite crack in the functionally graded materials under in-plane loading conditions reported by Ma et al. [23]. Menouillard et al. [24] solved the mixed-mode crack problems for the functionally graded materials. A numerical procedure based on the concept of the J-integral, for computation of the mixed-mode stress intensity factors for curved cracks, was obtained by Chang and Wu [25]. Dag et al. [26] studied the mixed-mode problem for an orthotropic functionally graded material under mechanical and thermal loading conditions. Using a dislocation-based approach, the modes I and II stress intensity factors for cracks and hoop stress for cavities in an orthotropic plane were obtained by Fotuhi and Fariborz [27]. Faal and Fariborz [28] employed distributed dislocation technique to analyze an orthotropic plane having multiple cracks. The results were used to evaluate modes I and II stress intensity factors. Fotuhi et al. [29] also provided the in-plane analysis of a cracked orthotropic half-plane. The problem of cracks in continuously nonhomogeneous medium studied by Sladek et al. [30]. They computed stress intensity factors at points far away from the crack tip. Hongmin et al. [31] adopted Wiener-Hopf technique to analyze the problem of semi-infinite cracks in an infinite functionally graded orthotropic material. Steady-state interaction between multiple cracks in an infinite plane under in-plane time-harmonic loads was studied by Ayatollahi and Fariborz [32]. Viscous damping can also be taken into account for analysis of defects studied by Mousavi and Fariborz [33]. Baghestani et al. [34] solved the mixed-mode problem of an orthotropic layer with multiple cracks.

The main advantage of method for the computation of stress intensity factors through the distributed dislocation technique is the applicability of the method to analysis of multiple cracks with arbitrary patterns in a functionally graded orthotropic half-plane. The stress fields in a functionally graded orthotropic half-plane caused by a climb and/or glide Volterra-type dislocation are obtained. The stress fields due to dislocations are then used to derive singular integral equations for a functionally graded orthotropic half-plane with multiple cracks under in-plane traction. For one straight crack in an infinite medium, the results match with those reported by Konda and Erdogan [9]. The effects of both crack interactions and the material parameters on the stress intensity factors k_I and k_{II} examined. The obtain results can be reduced to the solutions of crack problem of isotropic or orthotropic half-plane.

2 Formulation of the problem

Consider the plane problem of functionally graded orthotropic half-plane containing the Volterra edge dislocations. The constitutive relations of the functionally graded orthotropic materials may be written as

$$\begin{aligned}\sigma_{xx}(x, y) &= C_{11}(y)\varepsilon_{xx} + C_{12}(y)\varepsilon_{yy}, \\ \sigma_{yy}(x, y) &= C_{12}(y)\varepsilon_{xx} + C_{22}(y)\varepsilon_{yy}, \\ \sigma_{xy}(x, y) &= C_{66}(y)\gamma_{xy}.\end{aligned}\quad (1)$$

where $C_{11}(y)$, $C_{12}(y)$, $C_{22}(y)$ and $C_{66}(y)$ stand for the elastic stiffness constants of the FGMs and are based on a reasonable and generally accepted assumption that the material properties vary according to the following functions

$$C_{11}(y) = C_{110}e^{\beta y}, \quad C_{22}(y) = C_{220}e^{\beta y}, \quad C_{12}(y) = C_{120}e^{\beta y}, \quad C_{66}(y) = C_{660}e^{\beta y} \quad (2)$$

where β , C_{110} , C_{120} , C_{220} and C_{660} are constants. The stress components in terms of the stress function are given by

$$\sigma_{xx}(x, y) = \frac{\partial^2 f}{\partial y^2}, \quad \sigma_{yy}(x, y) = \frac{\partial^2 f}{\partial x^2}, \quad \sigma_{xy}(x, y) = -\frac{\partial^2 f}{\partial x \partial y} \quad (3)$$

The stress function f must satisfy the following differential equation

$$\frac{\partial^4 f}{\partial y^4} + \alpha_1 \frac{\partial^4 f}{\partial x^4} + \alpha_2 \frac{\partial^4 f}{\partial x^2 \partial y^2} - 2\beta \frac{\partial^3 f}{\partial y^3} + \beta^2 \frac{\partial^2 f}{\partial y^2} - \alpha_3 \beta^2 \frac{\partial^2 f}{\partial x^2} - \alpha_2 \beta \frac{\partial^3 f}{\partial x^2 \partial y} = 0. \quad (4)$$

where

$$\alpha_1 = \frac{C_{110}}{C_{220}}, \quad \alpha_2 = \frac{C_{110}C_{220} - C_{120}^2}{C_{220}C_{660}} - \frac{2C_{120}}{C_{220}} \quad \text{and} \quad \alpha_3 = \frac{C_{120}}{C_{220}}. \quad (5)$$

We consider the functionally graded orthotropic half-plane weakened by a glide and climb dislocations with Burgers vector b_x and b_y , respectively. A glide dislocation is an edge dislocation that can glide in x -direction, and its Burgers vector is in the x -direction. On the other hand, a climb dislocation can move only by climb in the x -direction and its Burgers vector is in the y -direction. Therefore, the conditions representing the dislocation are

$$\begin{aligned}u(x, 0^+) - u(x, 0^-) &= b_x H(x) \\ v(x, 0^+) - v(x, 0^-) &= b_y H(x)\end{aligned}\quad (6)$$

where $H(x)$ is the Heaviside step function. Moreover, for both types of dislocations, the following continuity of stress components along the x -axis should be satisfied. Consequently,

$$\begin{aligned}\sigma_{yy}(x, 0^+) &= \sigma_{yy}(x, 0^-), \\ \sigma_{xy}(x, 0^+) &= \sigma_{xy}(x, 0^-) \quad |x| < \infty.\end{aligned}\quad (7)$$

The traction-free conditions on the boundary of half-plane yield

$$\begin{aligned}\sigma_{yy}(x, h) &= 0, \\ \sigma_{xy}(x, h) &= 0.\end{aligned}\quad (8)$$

The solution of Eq. (4) is accomplished by means of the complex Fourier transform defined as

$$F(s, y) = \int_{-\infty}^{\infty} f(x, y) e^{isx} dx, \quad -\infty < x < \infty. \quad (9)$$

The application of Eqs. (9) to (4) with the aid of regularity condition $\lim_{|x| \rightarrow \infty} f(x, y) = 0$, leads to a fourth-order ordinary differential equation for $F(s, y)$. We obtain

$$\frac{d^4 F}{dy^4} - 2\beta \frac{d^3 F}{dy^3} + (\beta^2 - \alpha_2 s^2) \frac{d^2 F}{dy^2} + \alpha_2 \beta s^2 \frac{dF}{dy} + s^2 (\alpha_1 s^2 + \alpha_3 \beta^2) F = 0 \quad (10)$$

If we now also assume that $F = e^{\lambda y}$, we arrive at

$$\lambda^4 - 2\beta\lambda^3 + (\beta^2 - \alpha_2 s^2)\lambda^2 + \alpha_2\beta s^2\lambda + s^2(\alpha_1 s^2 + \alpha_3\beta^2) = 0 \quad (11)$$

It is seen that the characteristic Eq. (11) may be written as

$$\left(\lambda^2 - \beta\lambda - \frac{s^2\alpha_2}{2}\right)^2 + s^2 \left[\left(\alpha_1 - \frac{\alpha_2^2}{4}\right)s^2 + \alpha_3\beta^2\right] = 0 \quad (12)$$

The roots of the characteristic equation obtain from (12) as

$$\begin{aligned} \lambda_1 &= \frac{1}{2} \left[\beta - \sqrt{\beta^2 + 2\alpha_2 s^2 - 2\sqrt{s^4(\alpha_2^2 - 4\alpha_1) - 4s^2\beta^2\alpha_3}} \right], \quad Re[\lambda_1] < 0, \\ \lambda_2 &= \frac{1}{2} \left[\beta - \sqrt{\beta^2 + 2\alpha_2 s^2 + 2\sqrt{s^4(\alpha_2^2 - 4\alpha_1) - 4s^2\beta^2\alpha_3}} \right], \quad Re[\lambda_2] < 0, \\ \lambda_3 &= \frac{1}{2} \left[\beta + \sqrt{\beta^2 + 2\alpha_2 s^2 - 2\sqrt{s^4(\alpha_2^2 - 4\alpha_1) - 4s^2\beta^2\alpha_3}} \right], \quad Re[\lambda_3] > 0, \\ \lambda_4 &= \frac{1}{2} \left[\beta + \sqrt{\beta^2 + 2\alpha_2 s^2 + 2\sqrt{s^4(\alpha_2^2 - 4\alpha_1) - 4s^2\beta^2\alpha_3}} \right], \quad Re[\lambda_4] > 0. \end{aligned} \quad (13)$$

Since $f(x, y)$ must vanish for $r \rightarrow -\infty$, the solution of Eq. (10) in the Fourier transform domain become

$$\begin{aligned} F_1(s, y) &= A_1(s)e^{\lambda_1 y} + A_2(s)e^{\lambda_2 y} + A_3(s)e^{\lambda_3 y} + A_4(s)e^{\lambda_4 y}, \quad 0 < y < h, \\ F_2(s, y) &= A_5(s)e^{\lambda_3 y} + A_6(s)e^{\lambda_4 y}, \quad y < 0. \end{aligned} \quad (14)$$

The unknown coefficients in Eq. (14) are determined by utilizing the Fourier transforms of Eqs. (6)–(8). The expressions for these coefficients in a plane containing both dislocations are now determined as follows:

$$\begin{aligned} A_1(s) &= \frac{sC_{660}(\alpha_2 + 2\alpha_3)(\pi\delta(s) + i/s)}{(\lambda_1 - \lambda_2)(\lambda_1 - \lambda_3)(\lambda_1 - \lambda_4)} [sb_y + i\lambda_3 b_x] \\ A_2(s) &= -\frac{sC_{660}(\alpha_2 + 2\alpha_3)(\pi\delta(s) + i/s)}{(\lambda_1 - \lambda_2)(\lambda_2 - \lambda_3)(\lambda_2 - \lambda_4)} [sb_y + i\lambda_4 b_x] \\ A_3(s) &= \frac{sC_{660}(\alpha_2 + 2\alpha_3)(\pi\delta(s) + i/s)}{(\lambda_1 - \lambda_2)(\lambda_1 - \lambda_3)(\lambda_2 - \lambda_3)(\lambda_3 - \lambda_4)} \\ &\quad \times \left[(\lambda_1 - \lambda_3)(sb_y + i\lambda_4 b_x)e^{(\lambda_2 - \lambda_3)h} - (\lambda_2 - \lambda_3)(sb_y + i\lambda_3 b_x)e^{(\lambda_1 - \lambda_3)h} \right] \\ A_4(s) &= \frac{sC_{660}(\alpha_2 + 2\alpha_3)(\pi\delta(s) + i/s)}{(\lambda_1 - \lambda_2)(\lambda_4 - \lambda_3)(\lambda_2 - \lambda_4)(\lambda_1 - \lambda_4)} \\ &\quad \times \left[(\lambda_1 - \lambda_4)(sb_y + i\lambda_4 b_x)e^{(\lambda_2 - \lambda_4)h} - (\lambda_2 - \lambda_4)(sb_y + i\lambda_3 b_x)e^{(\lambda_1 - \lambda_4)h} \right] \\ A_5(s) &= -\frac{sC_{660}(\alpha_2 + 2\alpha_3)(\pi\delta(s) + i/s)}{(\lambda_1 - \lambda_2)(\lambda_3 - \lambda_4)(\lambda_2 - \lambda_3)(\lambda_1 - \lambda_3)} \\ &\quad \times \left[(\lambda_1 - \lambda_3)(sb_y + i\lambda_4 b_x)(1 - e^{(\lambda_2 - \lambda_3)h}) + (\lambda_2 - \lambda_3)(sb_y + i\lambda_3 b_x)(-1 + e^{(\lambda_1 - \lambda_3)h}) \right] \\ A_6(s) &= -\frac{sC_{660}(\alpha_2 + 2\alpha_3)(\pi\delta(s) + i/s)}{(\lambda_1 - \lambda_2)(\lambda_4 - \lambda_3)(\lambda_2 - \lambda_4)(\lambda_1 - \lambda_4)} \\ &\quad \times \left[(\lambda_1 - \lambda_4)(sb_y + i\lambda_4 b_x)(1 - e^{(\lambda_2 - \lambda_4)h}) + (\lambda_2 - \lambda_4)(sb_y + i\lambda_3 b_x)(-1 + e^{(\lambda_1 - \lambda_4)h}) \right] \end{aligned} \quad (15)$$

where $\delta(s)$ is the Dirac delta function. Substituting (15) into (14) and applying the inverse of Fourier transform and splitting into odd and even parts, furthermore, by taking $s = \beta\omega$, we arrive at

$$\begin{aligned}
f_1(x, y) &= \frac{C_{660}(\alpha_2 + 2\alpha_3)}{\pi\beta} \int_0^\infty \frac{1}{(r_1 - r_2)} \left\{ \left[\frac{r_4 e^{r_2 y \beta}}{(r_2 - r_3)(r_2 - r_4)} - \frac{r_3 e^{r_1 y \beta}}{(r_1 - r_3)(r_1 - r_4)} \right. \right. \\
&\quad + \frac{r_3(r_2 - r_3)e^{(r_1 - r_3)\beta h + r_3 y \beta} - r_4(r_1 - r_3)e^{(r_2 - r_3)\beta h + r_3 y \beta}}{(r_1 - r_3)(r_2 - r_3)(r_3 - r_4)} \\
&\quad + \left. \left. \frac{r_3(r_2 - r_4)e^{(r_1 - r_4)\beta h + r_4 y \beta} - r_4(r_1 - r_4)e^{(r_2 - r_4)\beta h + r_4 y \beta}}{(r_4 - r_3)(r_2 - r_4)(r_1 - r_4)} \right] \cos(\beta \omega x) b_x \right. \\
&\quad + \omega \left[\frac{e^{r_1 y \beta}}{(r_1 - r_3)(r_1 - r_4)} - \frac{e^{r_2 y \beta}}{(r_2 - r_3)(r_2 - r_4)} \right. \\
&\quad + \frac{(r_1 - r_3)e^{(r_2 - r_3)\beta h + r_3 y \beta} - (r_2 - r_3)e^{(r_1 - r_3)\beta h + r_3 y \beta}}{(r_1 - r_3)(r_2 - r_3)(r_3 - r_4)} \\
&\quad + \left. \left. \frac{(r_1 - r_4)e^{(r_2 - r_4)\beta h + r_4 y \beta} - (r_2 - r_4)e^{(r_1 - r_4)\beta h + r_4 y \beta}}{(r_4 - r_3)(r_2 - r_4)(r_1 - r_4)} \right] \sin(\beta \omega x) b_y \right\} d\omega, \quad 0 < y < h, \\
f_2(x, y) &= \frac{C_{660}(\alpha_2 + 2\alpha_3)}{\pi\beta} \int_0^\infty \frac{1}{(r_1 - r_2)(r_4 - r_3)} \\
&\quad \times \left\{ \left[\frac{r_3(r_2 - r_3)(1 - e^{(r_1 - r_3)\beta h}) - r_4(r_1 - r_3)(1 - e^{(r_2 - r_3)\beta h})}{(r_2 - r_3)(r_1 - r_3)} e^{r_3 y \beta} \right. \right. \\
&\quad + \left. \frac{r_4(r_1 - r_4)(1 - e^{(r_2 - r_4)\beta h}) - r_3(r_2 - r_4)(1 - e^{(r_1 - r_4)\beta h})}{(r_2 - r_4)(r_1 - r_4)} e^{r_4 y \beta} \right] \cos(\beta \omega x) b_x \\
&\quad + \omega \left[\frac{(r_1 - r_3)(1 - e^{(r_2 - r_3)\beta h}) - (r_2 - r_3)(1 - e^{(r_1 - r_3)\beta h})}{(r_2 - r_3)(r_1 - r_3)} e^{r_3 y \beta} \right. \\
&\quad + \left. \left. \frac{(r_2 - r_4)(1 - e^{(r_1 - r_4)\beta h}) - (r_1 - r_4)(1 - e^{(r_2 - r_4)\beta h})}{(r_2 - r_4)(r_1 - r_4)} e^{r_4 y \beta} \right] \sin(\beta \omega x) b_y \right\} ds, \quad y < 0.
\end{aligned} \tag{16}$$

where the expressions for r_i , $i = 1, 2, 3, 4$ are given by

$$\begin{aligned}
r_1 &= \frac{1}{2} \left[1 - \operatorname{sgn}(\beta) \sqrt{1 + 2\alpha_2 \omega^2 - 2\omega \sqrt{\omega^2 (\alpha_2^2 - 4\alpha_1) - 4\alpha_3}} \right], \\
r_2 &= \frac{1}{2} \left[1 - \operatorname{sgn}(\beta) \sqrt{1 + 2\alpha_2 \omega^2 + 2\omega \sqrt{\omega^2 (\alpha_2^2 - 4\alpha_1) - 4\alpha_3}} \right], \\
r_3 &= \frac{1}{2} \left[1 + \operatorname{sgn}(\beta) \sqrt{1 + 2\alpha_2 \omega^2 - 2\omega \sqrt{\omega^2 (\alpha_2^2 - 4\alpha_1) - 4\alpha_3}} \right], \\
r_4 &= \frac{1}{2} \left[1 + \operatorname{sgn}(\beta) \sqrt{1 + 2\alpha_2 \omega^2 + 2\omega \sqrt{\omega^2 (\alpha_2^2 - 4\alpha_1) - 4\alpha_3}} \right].
\end{aligned} \tag{17}$$

From (16) and (3), the stress components can be obtained as

$$\begin{aligned}
\sigma_{ij1}(x, y) &= \int_0^\infty H_{ij1}(x, y, \omega) d\omega, \quad 0 < y < h, \\
\sigma_{ij2}(x, y) &= \int_0^\infty H_{ij2}(x, y, \omega) d\omega, \quad y < 0.
\end{aligned} \tag{18}$$

The expressions for H_{ij1} , H_{ij2} , $i, j = x, y$ are given in ‘‘Appendix A.’’ In order to investigate and to separate a singular part of the stress components, the asymptotic behavior of the inner integral in Eq. (18) must be examined. Since the integrands are continuous functions of ω and also finite $\omega = 0$, we observe that the singularity must occur as ω goes to infinity. We determine the leading terms of Eq. (18) as $\omega \rightarrow \infty$. We may write Eq. (18) as follows:

$$\begin{aligned} \sigma_{ijk}(x, y) = & \int_0^{\infty} [H_{ijk}(x, y, \omega) - H_{ijk\infty}(x, y, \omega)]d\omega \\ & + \int_0^{\infty} H_{ijk\infty}(x, y, \omega)d\omega, \quad i, j = x, y, k = 1, 2. \end{aligned} \quad (19)$$

where $H_{ijk\infty}$ $i, j \in \{x, y\}$ is the asymptotic value of H_{ijk} for large value of ω . (‘‘Appendix B’’). The first integral in (19) is a bounded function in its domain of definition. After separating the singular parts of the kernels, we obtain

$$\begin{aligned} \begin{Bmatrix} \sigma_{xx1}(x, y) \\ \sigma_{yy1}(x, y) \\ \sigma_{xy1}(x, y) \end{Bmatrix} = & \frac{C_{660}(\alpha_2 + 2\alpha_3)e^{\frac{\beta y}{2}}}{2\pi (r_{11}^2 y^2 + x^2) (r_{22}^2 y^2 + x^2) (r_{11} + r_{22})} \begin{Bmatrix} y [(\alpha_2 + \sqrt{\alpha_1})x^2 + \alpha_1 y^2] \\ y [\sqrt{\alpha_1}y^2 - x^2] \\ x [\sqrt{\alpha_1}y^2 - x^2] \end{Bmatrix} b_x \\ & - \begin{Bmatrix} x [x^2 - \sqrt{\alpha_1}y^2] \\ \frac{x}{\sqrt{\alpha_1}} [(x^2 + (\alpha_2 + \sqrt{\alpha_1})y^2)] \\ y [x^2 - \sqrt{\alpha_1}y^2] \end{Bmatrix} b_y + \begin{Bmatrix} \int_0^{\infty} [H_{xx1}(x, y, \omega) - H_{xx1\infty}(x, y, \omega)]d\omega \\ \int_0^{\infty} [H_{yy1}(x, y, \omega) - H_{yy1\infty}(x, y, \omega)]d\omega \\ \int_0^{\infty} [H_{xy1}(x, y, \omega) - H_{xy1\infty}(x, y, \omega)]d\omega \end{Bmatrix}, \quad 0 < y < h, \\ \begin{Bmatrix} \sigma_{xx2}(x, y) \\ \sigma_{yy2}(x, y) \\ \sigma_{xy2}(x, y) \end{Bmatrix} = & \frac{C_{660}(\alpha_2 + 2\alpha_3)e^{\frac{\beta y}{2}}}{2\pi (r_{11}^2 y^2 + x^2) (r_{22}^2 y^2 + x^2) (r_{11} + r_{22})} \begin{Bmatrix} y [(\alpha_2 + \sqrt{\alpha_1})x^2 + \alpha_1 y^2] \\ y [\sqrt{\alpha_1}y^2 - x^2] \\ x [\sqrt{\alpha_1}y^2 - x^2] \end{Bmatrix} b_x \\ & - \begin{Bmatrix} x [x^2 - \sqrt{\alpha_1}y^2] \\ \frac{x}{\sqrt{\alpha_1}} [(x^2 + (\alpha_2 + \sqrt{\alpha_1})y^2)] \\ y [x^2 - \sqrt{\alpha_1}y^2] \end{Bmatrix} b_y + \begin{Bmatrix} \int_0^{\infty} [H_{xx2}(x, y, \omega) - H_{xx2\infty}(x, y, \omega)]d\omega \\ \int_0^{\infty} [H_{yy2}(x, y, \omega) - H_{yy2\infty}(x, y, \omega)]d\omega \\ \int_0^{\infty} [H_{xy2}(x, y, \omega) - H_{xy2\infty}(x, y, \omega)]d\omega \end{Bmatrix}, \quad y < 0. \end{aligned} \quad (20)$$

where

$$r_{11} = \operatorname{sgn}(\beta) \sqrt{\frac{\alpha_2}{2} - \sqrt{\left(\frac{\alpha_2}{2}\right)^2 - \alpha_1}}, \quad r_{22} = \operatorname{sgn}(\beta) \sqrt{\frac{\alpha_2}{2} + \sqrt{\left(\frac{\alpha_2}{2}\right)^2 - \alpha_1}}. \quad (21)$$

From Eq. (20), we may observe that stress components exhibit the familiar Cauchy-type singularity at dislocation location.

3 Formulation of multiple cracks

Distributed dislocation technique is a method to analyze a medium containing multiple cracks. Classical stress fields of the dislocations contain singularity which results in singular integral equations in distributed dislocation technique. The stress components caused by the climb and glide edge dislocations located at a point with coordinates (x_0, y_0) , read

$$\sigma_{ij}(x, y) = \begin{cases} k_{ij}^{11} (x - x_0, y - y_0) b_x + k_{ij}^{12} (x - x_0, y - y_0) b_y, & 0 < y < h, \\ k_{ij}^{21} (x - x_0, y - y_0) b_x + k_{ij}^{22} (x - x_0, y - y_0) b_y, & y < 0, \quad i, j = x, y. \end{cases} \quad (22)$$

in which k_{ij}^{lm} , $i, j = x, y, l, m = 1, 2$ are the coefficients of b_x and b_y and may be deduced from Eq. (20). Let N be the number of cracks in a functionally graded orthotropic half-plane. A curved crack in a functionally graded orthotropic half-plane may be described in parametric form as

$$\begin{aligned} x_i &= \alpha_i(s), \\ y_i &= \beta_i(s), \quad -1 \leq s \leq 1, \quad i \in \{1, 2, 3, \dots, N\}. \end{aligned} \quad (23)$$

The moveable orthogonal coordinate system (n, s) is chosen such that the origin may move on the crack, while s -axis remains tangent to the crack surface. Suppose climb and glide edge dislocations with unknown densities $B_{sk}(t)$ and $B_{nk}(t)$, respectively, are distributed on the segment $\sqrt{[\alpha'_i(t)]^2 + [\beta'_i(t)]^2} dt$ at the surface of i th crack, where $-1 \leq t \leq 1$ and the prime denotes differentiation with respect to the argument. Employing the principal of superposition, the components of traction vector at a point with coordinates $(\alpha_i(s), \beta_i(s))$, where parameter $-1 \leq s \leq 1$, on the surface of all cracks yield

$$\begin{aligned} \sigma_n(\alpha_k(s), \beta_k(s)) &= \sum_{k=1}^N \int_{-1}^1 [K_{11ik}(s, t)B_{sk}(t) + K_{12ik}(s, t)B_{nk}(t)] \sqrt{[\alpha'_k(t)]^2 + [\beta'_k(t)]^2} dt, \\ \sigma_s(\alpha_k(s), \beta_k(s)) &= \sum_{k=1}^N \int_{-1}^1 [K_{21ik}(s, t)B_{sk}(t) + K_{22ik}(s, t)B_{nk}(t)] \sqrt{[\alpha'_k(t)]^2 + [\beta'_k(t)]^2} dt, \quad -1 \leq s \leq 1. \end{aligned} \quad (24)$$

where the kernels in Eq. (24) are

$$\begin{aligned} K_{11ik}(s, t) &= \left\{ \frac{1}{2}k_{xx}^{l1}(x_i - x_k, y_i - y_k) \cos(\theta_i) (1 - \cos(2\theta_k)) \right. \\ &\quad + \frac{1}{2}k_{xx}^{l2}(x_i - x_k, y_i - y_k) \sin(\theta_i) (1 - \cos(2\theta_k)) \\ &\quad + \frac{1}{2}k_{yy}^{l1}(x_i - x_k, y_i - y_k) \cos(\theta_i) (1 + \cos(2\theta_k)) \\ &\quad + \frac{1}{2}k_{yy}^{l2}(x_i - x_k, y_i - y_k) \sin(\theta_i) (1 + \cos(2\theta_k)) \\ &\quad \left. - k_{xy}^{l1}(x_i - x_k, y_i - y_k) \cos(\theta_i) \sin(2\theta_k) - k_{xy}^{l2}(x_i - x_k, y_i - y_k) \sin(\theta_i) \sin(2\theta_k) \right\} \\ K_{12ik}(s, t) &= \left\{ -\frac{1}{2}k_{xx}^{l1}(x_i - x_k, y_i - y_k) \sin(\theta_i) (1 - \cos(2\theta_k)) \right. \\ &\quad + \frac{1}{2}k_{xx}^{l2}(x_i - x_k, y_i - y_k) \cos(\theta_i) (1 - \cos(2\theta_k)) \\ &\quad - \frac{1}{2}k_{yy}^{l1}(x_i - x_k, y_i - y_k) \sin(\theta_i) (1 + \cos(2\theta_k)) \\ &\quad + \frac{1}{2}k_{yy}^{l2}(x_i - x_k, y_i - y_k) \cos(\theta_i) (1 + \cos(2\theta_k)) \\ &\quad \left. + k_{xy}^{l1}(x_i - x_k, y_i - y_k) \sin(\theta_i) \sin(2\theta_k) - k_{xy}^{l2}(x_i - x_k, y_i - y_k) \cos(\theta_i) \sin(2\theta_k) \right\}, \\ K_{21ik}(s, t) &= \left\{ -\frac{1}{2}k_{xx}^{l1}(x_i - x_k, y_i - y_k) \cos(\theta_i) \sin(2\theta_k) - \frac{1}{2}k_{xx}^{l2}(x_i - x_k, y_i - y_k) \sin(\theta_i) \sin(2\theta_k) \right. \\ &\quad + \frac{1}{2}k_{yy}^{l1}(x_i - x_k, y_i - y_k) \cos(\theta_i) \sin(2\theta_k) + \frac{1}{2}k_{yy}^{l2}(x_i - x_k, y_i - y_k) \sin(\theta_i) \sin(2\theta_k) \\ &\quad \left. + k_{xy}^{l1}(x_i - x_k, y_i - y_k) \cos(\theta_i) \cos(2\theta_k) - k_{xy}^{l2}(x_i - x_k, y_i - y_k) \sin(\theta_i) \cos(2\theta_k) \right\}, \end{aligned}$$

$$\begin{aligned}
K_{22ik}(s, t) = & \left\{ \frac{1}{2}k_{xx}^{l1}(x_i - x_k, y_i - y_k) \sin(\theta_i) \sin(2\theta_k) - \frac{1}{2}k_{xx}^{l2}(x_i - x_k, y_i - y_k) \cos(\theta_i) \sin(2\theta_k) \right. \\
& - \frac{1}{2}k_{yy}^{l1}(x_i - x_k, y_i - y_k) \sin(\theta_i) \sin(2\theta_k) + \frac{1}{2}k_{yy}^{l2}(x_i - x_k, y_i - y_k) \cos(\theta_i) \sin(2\theta_k) \\
& \left. - k_{xy}^{l1}(x_i - x_k, y_i - y_k) \sin(\theta_i) \cos(2\theta_k) + k_{xy}^{l2}(x_i - x_k, y_i - y_k) \cos(\theta_i) \cos(2\theta_k) \right\}.
\end{aligned} \tag{25}$$

The analysis is straightforward and is not detailed here. The superscript $l = 1$ is for $0 < y < h$ and $l = 2$ for $y < 0$. The kernels in Eq. (24) exhibit Cauchy-type singularity for $i = k$ as $t \rightarrow s$. By the virtue of the Buckner's principle, the left side of Eq. (24), after changing the sign, is the traction caused by external loading on the uncracked medium at the presumed surfaces of cracks. Employing the definition of dislocation density function, the equations for the crack opening displacement across the i th crack yield

$$\begin{aligned}
u_{si}^+(s) - u_{si}^-(s) &= \int_{-1}^s \sqrt{[\alpha'_i(t)]^2 + [\beta'_i(t)]^2} [\cos(\theta_i(s) - \theta_i(t))B_{si}(t) + \sin(\theta_i(s) - \theta_i(t))B_{ni}(t)] dt, \\
u_{ni}^+(s) - u_{ni}^-(s) &= \int_{-1}^s \sqrt{[\alpha'_i(t)]^2 + [\beta'_i(t)]^2} [\cos(\theta_i(s) - \theta_i(t))B_{ni}(t) - \sin(\theta_i(s) - \theta_i(t))B_{si}(t)] dt, \\
i &\in \{1, 2, \dots, N\}
\end{aligned} \tag{26}$$

The displacement field is single valued out of an embedded crack surface. Consequently, the dislocation densities are subjected to the following closure requirements:

$$\begin{aligned}
\int_{-1}^1 \sqrt{[\alpha'_i(t)]^2 + [\beta'_i(t)]^2} [\cos(\theta_i(1) - \theta_i(t))B_{si}(t) + \sin(\theta_i(1) - \theta_i(t))B_{ni}(t)] dt &= 0, \\
\int_{-1}^1 \sqrt{[\alpha'_i(t)]^2 + [\beta'_i(t)]^2} [\cos(\theta_i(1) - \theta_i(t))B_{ni}(t) - \sin(\theta_i(1) - \theta_i(t))B_{si}(t)] dt &= 0, \quad i \in \{1, 2, \dots, N\}.
\end{aligned} \tag{27}$$

It is worth mentioning that the devised procedure despite its simplicity is capable of handling complicated crack arrangements. To evaluate the dislocation density, the Cauchy singular integral Eqs. (24) and (27) should be solved simultaneously. The stress fields near the crack tips have the singularity for the embedded cracks in a functionally graded orthotropic medium $1/\sqrt{r}$ where r is the distance from a crack tip. Therefore, the dislocation densities are taken as

$$\begin{aligned}
B_{si}(t) &= \frac{g_{si}(t)}{\sqrt{1-t^2}} \\
B_{ni}(t) &= \frac{g_{ni}(t)}{\sqrt{1-t^2}}, \quad -1 < t < 1, \quad i \in \{1, 2, \dots, N\}
\end{aligned} \tag{28}$$

Substituting Eq. (28) into Eqs. (27) and (24) and making use of the numerical solutions of integral equations with Cauchy-type kernel developed by Erdogan et al. [35] result in $g_{si}(t)$ and $g_{ni}(t)$. The modes I and II stress intensity factors for embedded cracks derived by Faal and Fariborz [28] are defined as,

$$\begin{aligned}
\begin{Bmatrix} K_{IL} \\ K_{IIL} \end{Bmatrix} &= \frac{\sqrt{2}(\alpha_2 + 2\alpha_3)}{4(r_{11} + r_{22})} \lim_{r_L \rightarrow 0} \frac{C_{66}(y)}{\sqrt{r_L}} \begin{Bmatrix} [u_n|_{\theta=\pi} - u_n|_{\theta=-\pi}]/r_{11}r_{22} \\ [u_s|_{\theta=\pi} - u_s|_{\theta=-\pi} \end{Bmatrix} \\
\begin{Bmatrix} K_{IR} \\ K_{IIR} \end{Bmatrix} &= \frac{\sqrt{2}(\alpha_2 + 2\alpha_3)}{4(r_{11} + r_{22})} \lim_{r_R \rightarrow 0} \frac{C_{66}(y)}{\sqrt{r_R}} \begin{Bmatrix} [u_n|_{\theta=\pi} - u_n|_{\theta=-\pi}]/r_{11}r_{22} \\ [u_s|_{\theta=\pi} - u_s|_{\theta=-\pi} \end{Bmatrix}
\end{aligned} \tag{29}$$

where the subscripts L and R designate to the left and right tips of crack, respectively, (Fig. 1), the geometry of crack implies

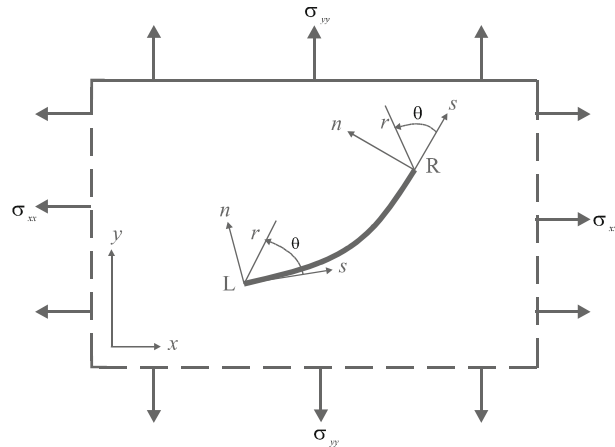


Fig. 1 Curved crack in a functionally graded orthotropic half-plane under biaxial loading

$$\begin{aligned}
 r_L &= [(\alpha_i(s) - \alpha_i(-1))^2 + (\beta_i(s) - \beta_i(-1))^2]^{\frac{1}{2}} \\
 r_R &= [(\alpha_i(s) - \alpha_i(1))^2 + (\beta_i(s) - \beta_i(1))^2]^{\frac{1}{2}}
 \end{aligned}
 \tag{30}$$

Substituting Eqs. (28) into (26), and results equations into (29) after using the Taylor series expansion of functions $\alpha_i(s)$ and $\beta_i(s)$ in the vicinity of the points $s = \pm 1$ leads to

$$\begin{aligned}
 \begin{Bmatrix} K_{IL} \\ K_{IIL} \end{Bmatrix} &= \frac{C_{660}(\alpha_2 + 2\alpha_3) \left([\alpha'_i(-1)]^2 + [\beta'_i(-1)]^2 \right)^{\frac{1}{4}}}{2(r_{11} + r_{22})} \begin{Bmatrix} g_{ni}(-1)/r_{11}r_{22} \\ g_{si}(-1) \end{Bmatrix} \\
 \begin{Bmatrix} K_{IR} \\ K_{IIR} \end{Bmatrix} &= -\frac{C_{660}(\alpha_2 + 2\alpha_3) \left([\alpha'_i(1)]^2 + [\beta'_i(1)]^2 \right)^{\frac{1}{4}}}{2(r_{11} + r_{22})} \begin{Bmatrix} g_{ni}(1)/r_{11}r_{22} \\ g_{si}(1) \end{Bmatrix}
 \end{aligned}
 \tag{31}$$

4 Numerical examples and discussion

In this section, numerical calculations are carried out. The validity of the approach is examined by solving some well-known problems whose solution has been previously obtained by other researchers. The analysis, developed in the preceding section, allows the consideration of a functionally graded orthotropic half-plane with multiple cracks subjected to in-plane tractions. The validation of the formulation is accomplished by comparing our results with Konda and Erdogan [9] by setting $h \rightarrow \infty$. The mixed-mode crack problem of functionally graded plane with a crack under constant normal traction has firstly been considered. Numerical results are given in Table 1. As it may be observed, the agreement of the results in the above example is reasonable. It is worth mentioning that, in the nonhomogeneous medium, in the stiffer portion of the materials, the crack surface displacement is smaller than that of the less stiff portion of the medium. It was found that the stress intensity factors increase with increasing the FG constant. Due to the lack of symmetry with respect to $y = 0$ plane, the stress state around crack tips is one of the mixed modes. In the remaining of this section, more examples are presented to demonstrate the applicability of the procedure.

Table 1 The effect of the nonhomogeneity constant on stress intensity factors for the case of plane strain

βa		0.1	0.25	0.5	1	2.5	5
K_I/K_0	Konda and Erdogan [9]	1.008	1.036	1.101	1.258	1.808	2.868
	Present	1.0085	1.0366	1.1015	1.2606	1.8163	2.8608
K_{II}/K_0	Konda and Erdogan [9]	0.026	0.065	0.129	0.263	0.697	1.567
	Present	0.025	0.0624	0.1255	0.2544	0.6743	1.4969

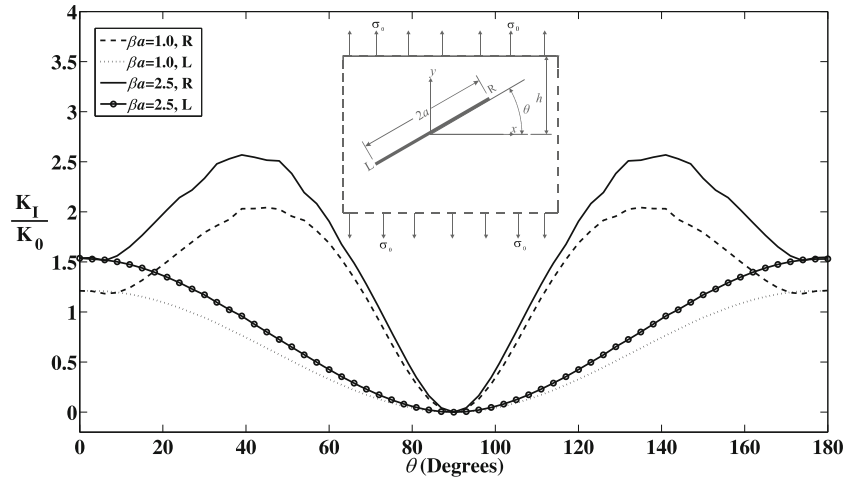


Fig. 2 Mode I stress intensity factor for a rotating crack

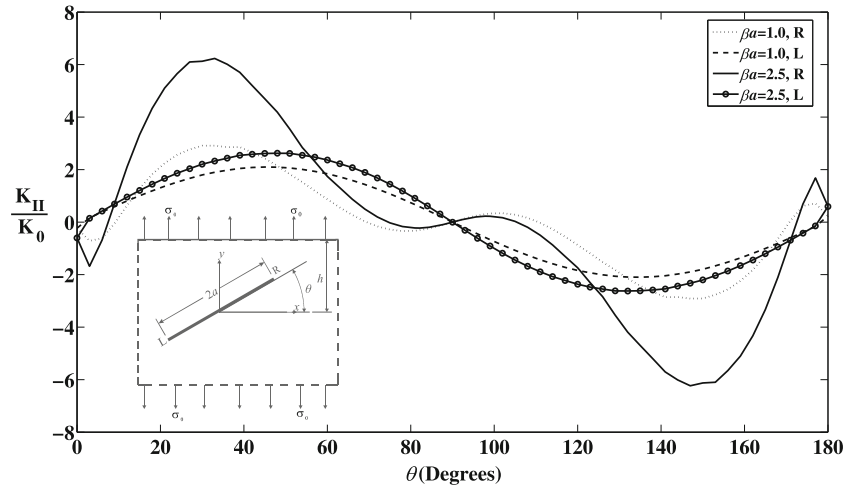


Fig. 3 Mode II stress intensity factors for a rotating crack

In the sequel, unless otherwise stated, the material properties for plane strain case are $C_{110} = 78.842$ GPa, $C_{120} = 3.003$ GPa, $C_{220} = 6.488$ GPa, $C_{660} = 2.070$ GPa Herakovich [36].

4.1 Straight crack with arbitrary orientation

The effect of nonhomogeneity constant on the stress intensity factors is shown in Figs. 2 and 3. The medium is under constant traction $\sigma_{yy} = \sigma_0$. The crack LR with length $2a = 2$ (cm) is an inclined crack with angle θ and centered at $(0, 0)$ for $h/a = 2.0$. The quantity for making the stress intensity factors dimensionless is $K_0 = \sigma_0\sqrt{a}$ where a is the half length of crack. The plots of the nondimensionalized modes I and II stress intensity factors versus crack orientation are shown. As physically expected, at $\theta = \pi/2$, the traction on the crack surface vanishes. Therefore, the stress intensity factors are zero. In order to investigate the effect of the nonhomogeneity constant on the modes I and II stress intensity factors, different values of β are studied. According to Figs 2 and 3, the influence of β is significant. It is interesting to note that for the crack tip which is located in a stiffer zone, the stress intensity factor is higher than the other tip. Also, the values of θ corresponding to maximum mode II stress intensity factors seem to depend on βa .

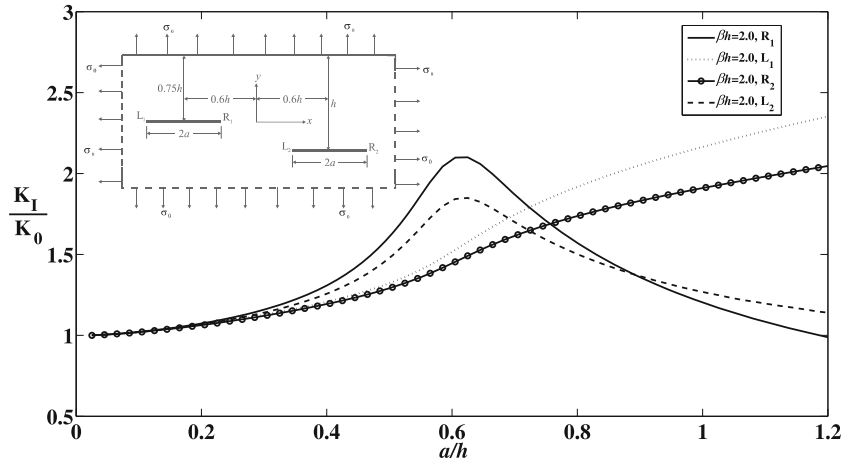


Fig. 4 Mode I stress intensity factors for two parallel off-center cracks

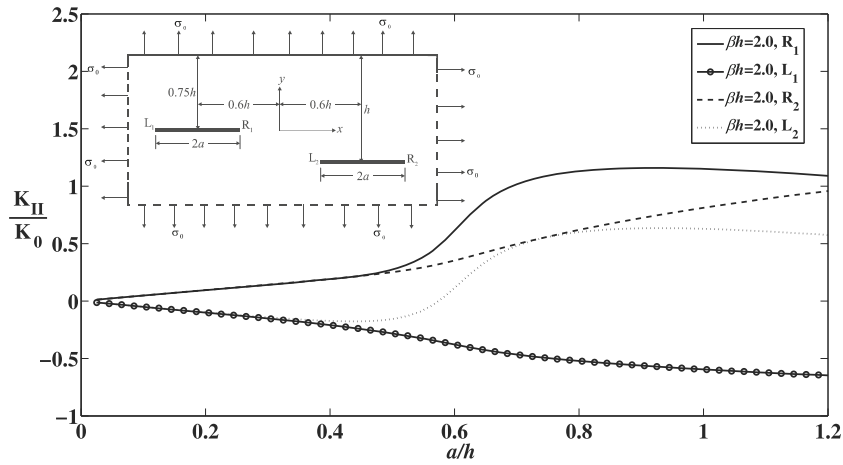


Fig. 5 Mode II stress intensity factors for two parallel off-center cracks

4.2 Two parallel off-center cracks

We consider two equal-length off-center cracks L_1R_1 and L_2R_2 as shown in Figs. 4 and 5. To ensure the opening of cracks with any configuration, the medium is subject to uniform biaxial traction $\sigma_{xx} = \sigma_0, \sigma_{yy} = \sigma_0$. The crack locations are fixed, whereas the crack lengths are changing with the same rates. The dimensionless modes I and II stress intensity factors are shown in Figs. 4 and 5. The value of FG constant is taken $\beta h = 2.0$. Obviously, the values of stress intensity factors are under the effect of FG constant, but the trend of variations remains the same by changing the FG constant.

4.3 A straight and a circular arc crack

The next example deals with the interaction of a straight and a circular arc crack, as shown in Figs. 6 and 7. The parametric representations of straight and circular arc cracks are, respectively,

$$\begin{aligned}
 \alpha_1(t) &= 2a + lt, \\
 \beta_1(t) &= 0, \\
 \alpha_2(t) &= a \cos(\varphi t), \\
 \beta_2(t) &= a \sin(\varphi t), \quad -1 \leq t \leq 1.
 \end{aligned}
 \tag{32}$$

The center of straight crack is fixed, but its length is changing. As it was expected, the modes I and II stress intensity factors of the crack tips increase by increasing the length of the straight cracks. The magnitudes of

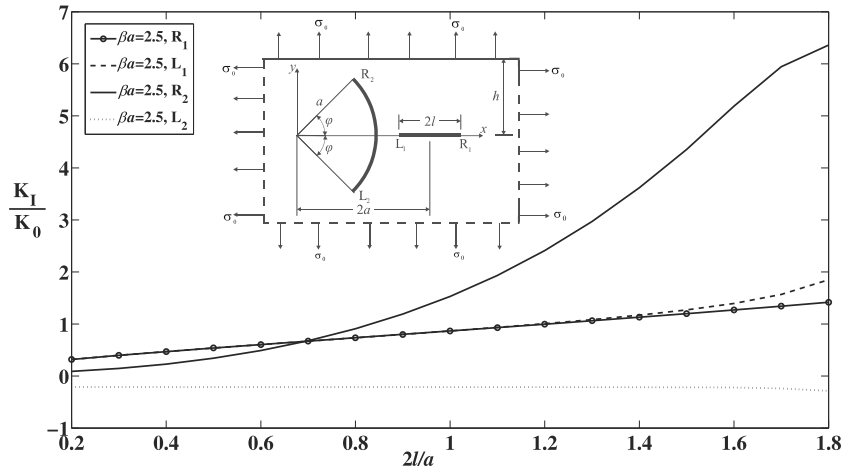


Fig. 6 Mode I stress intensity factors of a straight and a circular arc crack

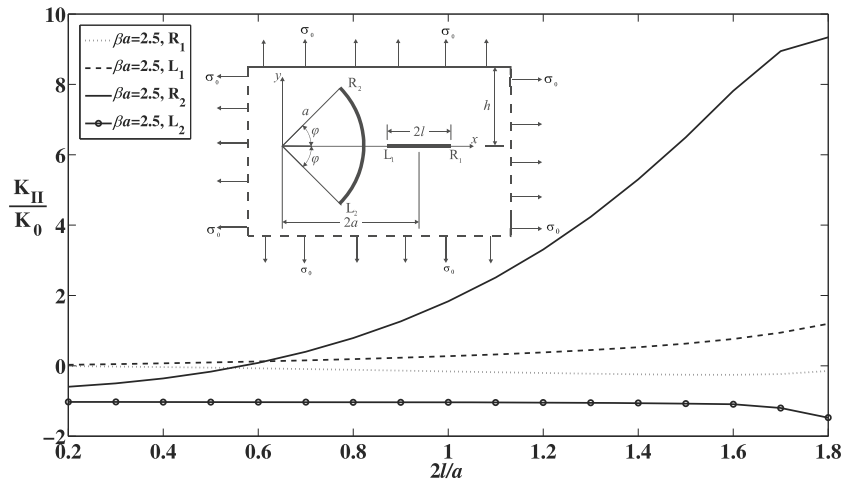


Fig. 7 Mode II stress intensity factors of a straight and a circular arc crack

SIFs at crack tip L_1 are larger than those at the tip R_1 , because L_1 has stronger interaction with the curved crack. Also, we observed that the crack opening displacement at the crack tip with smaller material properties is higher than the other tip located in higher material properties region. However, the overall effects result in a higher stress intensity factors for crack tip R_2 which is located in a stiffer zone. We may conclude that the effect of material nonhomogeneity is more significant.

4.4 Two circular arc cracks

As the last example, we consider two circular arc cracks which are portions of the circumference of a circle. The half-plane is under uniform biaxial traction $\sigma_{xx} = \sigma_0, \sigma_{yy} = \sigma_0$ (Figs. 8 and 9). The cracks may be represented in the following parametric forms

$$\begin{aligned} \alpha_i(t) &= a_i \cos(\varphi t), \\ \beta_i(t) &= a_i \sin(\varphi t), \quad -1 \leq t \leq 1, i = 1, 2. \end{aligned} \tag{33}$$

Figures 8 and 9 show the variation of dimensionless modes I and II stress intensity factors versus angle φ . The centers of cracks remain fixed, while the crack lengths are changing. As it may be observed, the maximum stress intensity factor for a crack tips occurs when the crack length is increased. Due to interaction with the boundary of the half-plane, the intensity factors at R are higher than those at L .

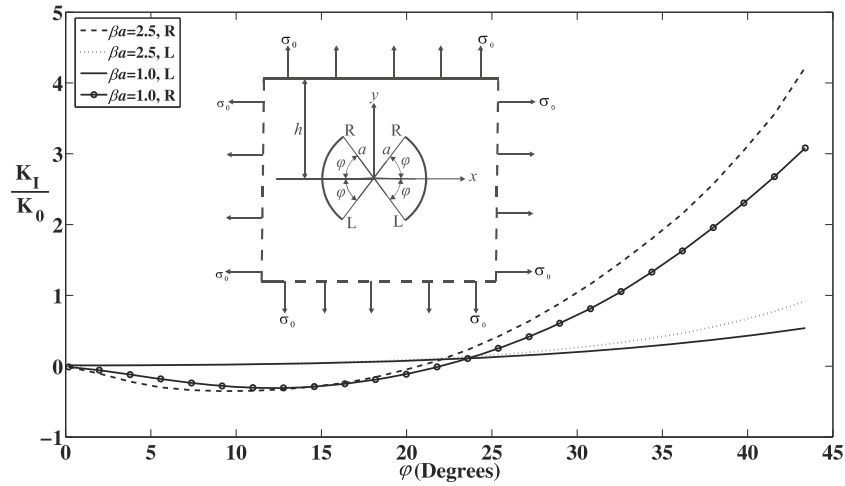


Fig. 8 Mode I stress intensity factors of two curved cracks

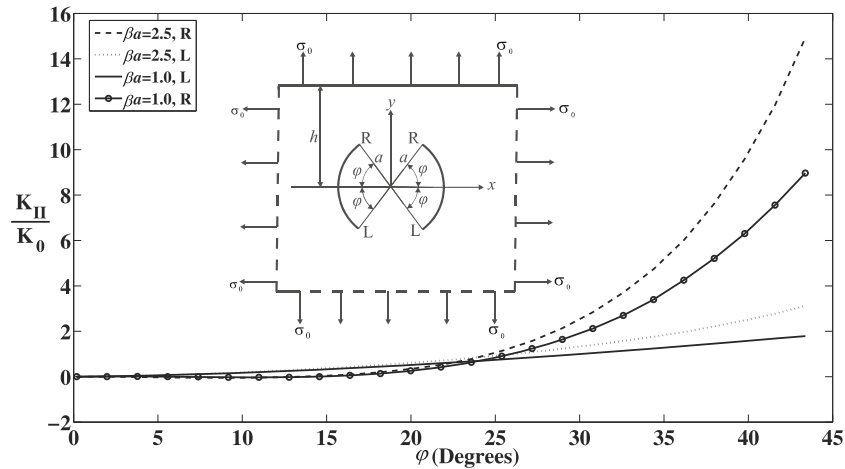


Fig. 9 Mode II stress intensity factors of two curved cracks

5 Conclusions

In this paper, the multiple cracks problem in a functionally graded orthotropic half-plane under mixed-mode condition is investigated. A solution for the stress field caused by the Volterra-type climb and glide edge dislocations in a functionally graded orthotropic half-plane is first obtained. In the particular case of the functionally graded plane, the solutions are in accordance with the well-known results in the literature. The stress components are used as the Green’s function to derive integral equations for the analysis of multiple cracks. Several examples are solved, and modes I and II stress intensity factors are determined for interacting cracks.

Appendix A

The integrands of Eq. (18) are given as

$$\begin{aligned}
 H_{xx1}(x, y, \omega) = & \frac{\beta C_{660}(\alpha_2 + 2\alpha_3)}{\pi} \frac{1}{(r_1 - r_2)} \left\{ b_x \left[\frac{r_4 r_2^2 e^{r_2 y \beta}}{(r_2 - r_3)(r_2 - r_4)} - \frac{r_3 r_2^2 e^{r_1 y \beta}}{(r_1 - r_3)(r_1 - r_4)} \right] \right. \\
 & \left. + \frac{r_3^3 (r_2 - r_3) e^{(r_1 - r_3)\beta h + r_3 y \beta} - r_4 r_3^2 (r_1 - r_3) e^{(r_2 - r_3)\beta h + r_3 y \beta}}{(r_1 - r_3)(r_2 - r_3)(r_3 - r_4)} \right\}
 \end{aligned}$$

$$\begin{aligned}
& + \frac{r_3 r_4^2 (r_2 - r_4) e^{(r_1 - r_4)\beta h + r_4 y \beta} - r_4^3 (r_1 - r_4) e^{(r_2 - r_4)\beta h + r_4 y \beta}}{(r_4 - r_3)(r_2 - r_4)(r_1 - r_4)} \Big] \cos(\beta \omega x) \\
& + \omega b_y \left[\frac{r_1^2 e^{r_1 y \beta}}{(r_1 - r_3)(r_1 - r_4)} - \frac{r_2^2 e^{r_2 y \beta}}{(r_2 - r_3)(r_2 - r_4)} \right. \\
& + \frac{r_3^2 (r_1 - r_3) e^{(r_2 - r_3)\beta h + r_3 y \beta} - r_3^2 (r_2 - r_3) e^{(r_1 - r_3)\beta h + r_3 y \beta}}{(r_1 - r_3)(r_2 - r_3)(r_3 - r_4)} \\
& \left. + \frac{r_4^2 (r_1 - r_4) e^{(r_2 - r_4)\beta h + r_4 y \beta} - r_4^2 (r_2 - r_4) e^{(r_1 - r_4)\beta h + r_4 y \beta}}{(r_4 - r_3)(r_2 - r_4)(r_1 - r_4)} \right] \sin(\beta \omega x) \Big\}, \quad (34)
\end{aligned}$$

$$\begin{aligned}
H_{yy1}(x, y, \omega) = & - \frac{\beta C_{660}(\alpha_2 + 2\alpha_3)}{\pi} \frac{\omega^2}{(r_1 - r_2)} \left\{ b_x \left[\frac{r_4 e^{r_2 y \beta}}{(r_2 - r_3)(r_2 - r_4)} - \frac{r_3 e^{r_1 y \beta}}{(r_1 - r_3)(r_1 - r_4)} \right. \right. \\
& + \frac{r_3 (r_2 - r_3) e^{(r_1 - r_3)\beta h + r_3 y \beta} - r_4 (r_1 - r_3) e^{(r_2 - r_3)\beta h + r_3 y \beta}}{(r_1 - r_3)(r_2 - r_3)(r_3 - r_4)} \\
& \left. + \frac{r_3 (r_2 - r_4) e^{(r_1 - r_4)\beta h + r_4 y \beta} - r_4 (r_1 - r_4) e^{(r_2 - r_4)\beta h + r_4 y \beta}}{(r_4 - r_3)(r_2 - r_4)(r_1 - r_4)} \right] \cos(\beta \omega x) \\
& + \omega b_y \left[\frac{e^{r_1 y \beta}}{(r_1 - r_3)(r_1 - r_4)} - \frac{e^{r_2 y \beta}}{(r_2 - r_3)(r_2 - r_4)} \right. \\
& + \frac{(r_1 - r_3) e^{(r_2 - r_3)\beta h + r_3 y \beta} - (r_2 - r_3) e^{(r_1 - r_3)\beta h + r_3 y \beta}}{(r_1 - r_3)(r_2 - r_3)(r_3 - r_4)} \\
& \left. + \frac{(r_1 - r_4) e^{(r_2 - r_4)\beta h + r_4 y \beta} - (r_2 - r_4) e^{(r_1 - r_4)\beta h + r_4 y \beta}}{(r_4 - r_3)(r_2 - r_4)(r_1 - r_4)} \right] \sin(\beta \omega x) \Big\}, \quad (35)
\end{aligned}$$

$$\begin{aligned}
H_{xy1}(x, y, \omega) = & \frac{\beta C_{660}(\alpha_2 + 2\alpha_3)}{\pi} \frac{\omega}{(r_1 - r_2)} \left\{ b_x \left[\frac{r_2 r_4 e^{r_2 y \beta}}{(r_2 - r_3)(r_2 - r_4)} - \frac{r_1 r_3 e^{r_1 y \beta}}{(r_1 - r_3)(r_1 - r_4)} \right. \right. \\
& + \frac{r_3^2 (r_2 - r_3) e^{(r_1 - r_3)\beta h + r_3 y \beta} - r_3 r_4 (r_1 - r_3) e^{(r_2 - r_3)\beta h + r_3 y \beta}}{(r_1 - r_3)(r_2 - r_3)(r_3 - r_4)} \\
& \left. + \frac{r_3 r_4 (r_2 - r_4) e^{(r_1 - r_4)\beta h + r_4 y \beta} - r_4^2 (r_1 - r_4) e^{(r_2 - r_4)\beta h + r_4 y \beta}}{(r_4 - r_3)(r_2 - r_4)(r_1 - r_4)} \right] \sin(\beta \omega x) \\
& - \omega b_y \left[\frac{r_1 e^{r_1 y \beta}}{(r_1 - r_3)(r_1 - r_4)} - \frac{r_2 e^{r_2 y \beta}}{(r_2 - r_3)(r_2 - r_4)} \right. \\
& + \frac{r_3 (r_1 - r_3) e^{(r_2 - r_3)\beta h + r_3 y \beta} - r_3 (r_2 - r_3) e^{(r_1 - r_3)\beta h + r_3 y \beta}}{(r_1 - r_3)(r_2 - r_3)(r_3 - r_4)} \\
& \left. + \frac{r_4 (r_1 - r_4) e^{(r_2 - r_4)\beta h + r_4 y \beta} - r_4 (r_2 - r_4) e^{(r_1 - r_4)\beta h + r_4 y \beta}}{(r_4 - r_3)(r_2 - r_4)(r_1 - r_4)} \right] \cos(\beta \omega x) \Big\}, \quad (36)
\end{aligned}$$

$$\begin{aligned}
H_{xx2}(x, y, \omega) = & \frac{\beta C_{660}(\alpha_2 + 2\alpha_3)}{\pi} \frac{1}{(r_1 - r_2)(r_4 - r_3)} \left\{ b_x \left[\frac{r_3^3 (r_2 - r_3)(1 - e^{(r_1 - r_3)\beta h}) - r_4 r_3^2 (r_1 - r_3)(1 - e^{(r_2 - r_3)\beta h})}{(r_2 - r_3)(r_1 - r_3)} e^{r_3 y \beta} \right. \right. \\
& + \frac{r_4^3 (r_1 - r_4)(1 - e^{(r_2 - r_4)\beta h}) - r_3 r_4^2 (r_2 - r_4)(1 - e^{(r_1 - r_4)\beta h})}{(r_2 - r_4)(r_1 - r_4)} e^{r_4 y \beta} \Big] \cos(\beta \omega x) \\
& + \omega b_y \left[\frac{r_3^2 (r_1 - r_3)(1 - e^{(r_2 - r_3)\beta h}) - r_3^2 (r_2 - r_3)(1 - e^{(r_1 - r_3)\beta h})}{(r_2 - r_3)(r_1 - r_3)} e^{r_3 y \beta} \right. \\
& \left. + \frac{r_4^2 (r_2 - r_4)(1 - e^{(r_1 - r_4)\beta h}) - r_4^2 (r_1 - r_4)(1 - e^{(r_2 - r_4)\beta h})}{(r_2 - r_4)(r_1 - r_4)} e^{r_4 y \beta} \right] \sin(\beta \omega x) \Big\}, \quad (37)
\end{aligned}$$

$$\begin{aligned}
H_{yy2}(x, y, \omega) = & -\frac{\beta C_{660}(\alpha_2 + 2\alpha_3)}{\pi} \frac{\omega^2}{(r_1 - r_2)(r_4 - r_3)} \left\{ b_x \left[\frac{r_3(r_2 - r_3)(1 - e^{(r_1-r_3)\beta h}) - r_4(r_1 - r_3)(1 - e^{(r_2-r_3)\beta h})}{(r_2 - r_3)(r_1 - r_3)} e^{r_3 y \beta} \right. \right. \\
& + \left. \frac{r_4(r_1 - r_4)(1 - e^{(r_2-r_4)\beta h}) - r_3(r_2 - r_4)(1 - e^{(r_1-r_4)\beta h})}{(r_2 - r_4)(r_1 - r_4)} e^{r_4 y \beta} \right] \cos(\beta \omega x) \\
& + \omega b_y \left[\frac{(r_1 - r_3)(1 - e^{(r_2-r_3)\beta h}) - (r_2 - r_3)(1 - e^{(r_1-r_3)\beta h})}{(r_2 - r_3)(r_1 - r_3)} e^{r_3 y \beta} \right. \\
& + \left. \frac{(r_2 - r_4)(1 - e^{(r_1-r_4)\beta h}) - (r_1 - r_4)(1 - e^{(r_2-r_4)\beta h})}{(r_2 - r_4)(r_1 - r_4)} e^{r_4 y \beta} \right] \sin(\beta \omega x) \left. \right\}, \quad (38)
\end{aligned}$$

$$\begin{aligned}
H_{xy2}(x, y, \omega) = & \frac{\beta C_{660}(\alpha_2 + 2\alpha_3)}{\pi} \frac{\omega}{(r_1 - r_2)(r_4 - r_3)} \left\{ b_x \left[\frac{r_3^2(r_2 - r_3)(1 - e^{(r_1-r_3)\beta h}) - r_3 r_4(r_1 - r_3)(1 - e^{(r_2-r_3)\beta h})}{(r_2 - r_3)(r_1 - r_3)} e^{r_3 y \beta} \right. \right. \\
& + \left. \frac{r_4^2(r_1 - r_4)(1 - e^{(r_2-r_4)\beta h}) - r_3 r_4(r_2 - r_4)(1 - e^{(r_1-r_4)\beta h})}{(r_2 - r_4)(r_1 - r_4)} e^{r_4 y \beta} \right] \sin(\beta \omega x) \\
& - \omega b_y \left[\frac{r_3(r_1 - r_3)(1 - e^{(r_2-r_3)\beta h}) - r_3(r_2 - r_3)(1 - e^{(r_1-r_3)\beta h})}{(r_2 - r_3)(r_1 - r_3)} e^{r_3 y \beta} \right. \\
& + \left. \frac{r_4(r_2 - r_4)(1 - e^{(r_1-r_4)\beta h}) - r_4(r_1 - r_4)(1 - e^{(r_2-r_4)\beta h})}{(r_2 - r_4)(r_1 - r_4)} e^{r_4 y \beta} \right] \cos(\beta \omega x) \left. \right\}. \quad (39)
\end{aligned}$$

Appendix B

$$\begin{aligned}
H_{xx1\infty}(x, y, \omega) = & \frac{\beta C_{660}(\alpha_2 + 2\alpha_3)e^{\frac{y\beta}{2}}}{2\pi(r_{11} - r_{22})(r_{11} + r_{22})} \left[(r_{11}^2 e^{-r_{11}y\beta\omega} - r_{22}^2 e^{-r_{22}y\beta\omega}) \cos(\beta x \omega) b_x \right. \\
& \left. - (r_{11} e^{-r_{11}y\beta\omega} - r_{22} e^{-r_{22}y\beta\omega}) \sin(\beta x \omega) b_y \right], \quad (40)
\end{aligned}$$

$$\begin{aligned}
H_{yy1\infty}(x, y, \omega) = & -\frac{\beta C_{660}(\alpha_2 + 2\alpha_3)e^{\frac{y\beta}{2}}}{2\pi(r_{11} - r_{22})(r_{11} + r_{22})} \left[(e^{-r_{11}y\beta\omega} - e^{-r_{22}y\beta\omega}) \cos(\beta x \omega) b_x \right. \\
& \left. - \left(\frac{e^{-r_{11}y\beta\omega}}{r_{11}} - \frac{e^{-r_{22}y\beta\omega}}{r_{22}} \right) \sin(\beta x \omega) b_y \right], \quad (41)
\end{aligned}$$

$$\begin{aligned}
H_{xy1\infty}(x, y, \omega) = & -\frac{\beta C_{660}(\alpha_2 + 2\alpha_3)e^{\frac{y\beta}{2}}}{2\pi(r_{11} - r_{22})(r_{11} + r_{22})} \left[(r_{11} e^{-r_{11}y\beta\omega} - r_{22} e^{-r_{22}y\beta\omega}) \sin(\beta x \omega) b_x \right. \\
& \left. + (e^{-r_{11}y\beta\omega} - e^{-r_{22}y\beta\omega}) \cos(\beta x \omega) b_y \right], \quad (42)
\end{aligned}$$

$$\begin{aligned}
H_{xx2\infty}(x, y, \omega) = & -\frac{\beta C_{660}(\alpha_2 + 2\alpha_3)e^{\frac{y\beta}{2}}}{2\pi(r_{11} - r_{22})(r_{11} + r_{22})} \left[(r_{11}^2 e^{r_{11}y\beta\omega} - r_{22}^2 e^{r_{22}y\beta\omega}) \cos(\beta x \omega) b_x \right. \\
& \left. + (r_{11} e^{r_{11}y\beta\omega} - r_{22} e^{r_{22}y\beta\omega}) \sin(\beta x \omega) b_y \right], \quad (43)
\end{aligned}$$

$$\begin{aligned}
H_{yy2\infty}(x, y, \omega) = & \frac{\beta C_{660}(\alpha_2 + 2\alpha_3)e^{\frac{y\beta}{2}}}{2\pi(r_{11} - r_{22})(r_{11} + r_{22})} \left[(e^{r_{11}y\beta\omega} - e^{r_{22}y\beta\omega}) \cos(\beta x \omega) b_x \right. \\
& \left. + \left(\frac{e^{r_{11}y\beta\omega}}{r_{11}} - \frac{e^{r_{22}y\beta\omega}}{r_{22}} \right) \sin(\beta x \omega) b_y \right], \quad (44)
\end{aligned}$$

$$\begin{aligned}
H_{xy2\infty}(x, y, \omega) = & -\frac{\beta C_{660}(\alpha_2 + 2\alpha_3)e^{\frac{y\beta}{2}}}{2\pi(r_{11} - r_{22})(r_{11} + r_{22})} \left[(r_{11} e^{r_{11}y\beta\omega} - r_{22} e^{r_{22}y\beta\omega}) \sin(\beta x \omega) b_x \right. \\
& \left. - (e^{r_{11}y\beta\omega} - e^{r_{22}y\beta\omega}) \cos(\beta x \omega) b_y \right]. \quad (45)
\end{aligned}$$

References

1. Erdogan, F.: Stress distribution in a non-homogeneous elastic plane with cracks. *J. Appl. Mech. Trans. ASME* **30**, 232–236 (1963)
2. Karihaloo, B.L.: Spread of plasticity from stacked stress concentrations. *Int. J. Solids Struct.* **13**, 221–228 (1977)
3. Karihaloo, B.L.: Fracture characteristics of solids containing doubly-periodic arrays of cracks. *Proc. R. Soc. Lond. A* **360**, 373–387 (1978)
4. Karihaloo, B.L.: Fracture of solids containing arrays of cracks. *Eng. Fract. Mech.* **12**, 49–77 (1979)
5. Delale, F., Erdogan, F.: Crack problem for a non-homogeneous plane. *J. Appl. Mech.* **50**, 609–614 (1983)
6. Delale, F., Erdogan, F.: Interface crack in a nonhomogeneous elastic medium. *Int. J. Eng. Sci.* **26**, 559–568 (1988)
7. Erdogan, F., Kaya, A.C., Joseph, P.F.: The crack problem in bonded nonhomogeneous materials. *J. Appl. Mech. Trans. ASME* **58**, 410–418 (1991)
8. Ozturk, M., Erdogan, F.: The axisymmetric crack problem in a nonhomogeneous medium. *J. Appl. Mech. Trans. ASME* **60**, 406–413 (1993)
9. Konda, N., Erdogan, F.: The mixed mode crack problem in a nonhomogeneous elastic medium. *Eng. Fract. Mech.* **47**, 533–545 (1994)
10. Mauge, C., Kachanov, M.: Anisotropic material with interacting arbitrarily oriented cracks stress intensity factors and crack-microcrack interactions. *Int. J. Fract.* **65**, 115–139 (1994)
11. Erdogan, F.: Fracture mechanics of functionally graded materials. *Compos. Eng.* **5**, 753–770 (1995)
12. Chen, Y.F., Erdogan, F.: The interface crack problem for a nonhomogeneous coating bonded to homogeneous substrate. *J. Mech. Phys. Solids* **44**, 771–787 (1996)
13. Jin, Z.H., Batra, R.C.: Some basic fracture mechanics concepts in functionally graded materials. *J. Mech. Phys. Solids* **44**, 1221–1235 (1996)
14. Gu, P., Asaro, R.J.: Cracks in functionally graded materials. *Int. J. Solids Struct.* **34**, 1–17 (1997)
15. Ozturk, M., Erdogan, F.: Mode I crack problem in an inhomogeneous orthotropic medium. *Int. J. Eng. Sci.* **35**, 869–883 (1997)
16. Ozturk, M., Erdogan, F.: The mixed mode crack problem in an inhomogeneous orthotropic medium. *Int. J. Fract.* **98**, 243–261 (1999)
17. Anlas, G., Santare, M.H., Lambros, J.: Numerical calculation of stress intensity factors in functionally graded materials. *Int. J. Fract.* **104**, 131–143 (2000)
18. Huang, H., Kardomateas, G.A.: Stress intensity factors for a mixed mode center crack in an anisotropic strip. *Int. J. Fract.* **108**, 367–381 (2001)
19. Dolbow, J.E., Gosz, M.: On the computation of mixed-mode stress intensity factors in functionally graded materials. *Int. J. Solids Struct.* **39**, 2557–2574 (2002)
20. Wang, L.B., Mai, Y.W., Sun, Y.G.: Fracture mechanics analysis model for functionally graded materials with arbitrarily distributed properties. *Int. J. Fract.* **116**, 161–177 (2002)
21. Guo, L.C., Wu, L.Z., Zeng, T., Ma, L.: Mode I crack problem for a functionally graded orthotropic strip. *Eur. J. Mech. A Solids* **23**, 219–234 (2004)
22. Long, X., Delale, F.: The mixed mode crack problem in an FGM layer bonded to a homogeneous half-plane. *Int. J. Solids Struct.* **42**, 3897–3917 (2005)
23. Ma, L., Wu, L.Z., Guo, L.C., Zhou, Z.G.: Dynamic behavior of a finite crack in the functionally graded materials. *Mech. Mater.* **37**, 1153–1165 (2005)
24. Menouillard, T., Elguedj, T., Combescure, A.: Mixed mode stress intensity factors for graded materials. *Int. J. Solids Struct.* **43**, 1946–1959 (2006)
25. Chang, J.H., Wu, D.J.: Computation of mixed-mode stress intensity factors for curved cracks in anisotropic elastic solids. *Eng. Fract. Mech.* **74**, 1360–1372 (2007)
26. Dag, S., Yildirim, B., Sarikaya, D.: Mixed-mode fracture analysis of orthotropic functionally graded materials under mechanical and thermal loads. *Int. J. Solids Struct.* **44**, 7816–7840 (2007)
27. Fotuhi, A.R., Fariborz, S.J.: In-plane stress analysis of an orthotropic plane containing multiple defects. *Int. J. Solids Struct.* **44**, 4167–4183 (2007)
28. Faal, R.T., Fariborz, S.J.: Stress analysis of orthotropic planes weakened by cracks. *Appl. Math. Model.* **31**, 1133–1148 (2007)
29. Fotuhi, A.R., Faal, R.T., Fariborz, S.J.: In-plane analysis of a cracked orthotropic half-plane. *Int. J. Solids Struct.* **44**, 1608–1627 (2007)
30. Sladek, J., Sladek, V., Zhang, C.H.: Evaluation of the stress intensity factors for cracks in continuously non-homogeneous solids, Part I: interaction integral. *Mech. Adv. Mater. Struct.* **15**, 438–443 (2008)
31. Hongmin, X., Xuefeng, Y., Xiqiao, F., Yeh, H.Y.: Dynamic stress intensity factors of a semi-infinite crack in an orthotropic functionally graded material. *Mech. Mater.* **40**, 37–47 (2008)
32. Ayatollahi, M., Fariborz, S.J.: Elastodynamic analysis of a plane weakened by several cracks. *Int. J. Solids Struct.* **46**, 1743–1754 (2009)
33. Mousavi, S.M., Fariborz, S.J.: Anti-plane elastodynamic analysis of cracked graded orthotropic layers with viscous damping. *Appl. Math. Model.* **36**, 1626–1638 (2012)
34. Baghestani, A.M., Fotuhi, A.R., Fariborz, S.J.: Multiple interacting cracks in an orthotropic layer. *Arch. Appl. Mech.* **83**, 1549–1567 (2013)
35. Erdogan, F., Gupta, G.D., Cook, T.S.: Numerical solution of integral equations. In: Sih, G.C. *Methods of Analysis and Solution of Crack Problems*. Noordhoff, Leyden, Holland (1973)
36. Herakovich, C.T.: *Mechanics of Fibrous Composites*. Wiley, New York (1997)